



Dalton  
Transactions

**Myoglobins engineered with artificial cofactors serve as  
artificial metalloenzymes and models of natural enzymes**

Journal:	<i>Dalton Transactions</i>
Manuscript ID	DT-PER-10-2020-003597.R1
Article Type:	Perspective
Date Submitted by the Author:	18-Dec-2020
Complete List of Authors:	Oohora, Koji; Osaka University, Applied Chemistry Hayashi, Takashi; Osaka University, Applied Chemistry

SCHOLARONE™  
Manuscripts

## ARTICLE

# Myoglobins engineered with artificial cofactors serve as artificial metalloenzymes and models of natural enzymes

Koji Oohora,\* and Takashi Hayashi\*

Received 00th January 20xx,  
Accepted 00th January 20xx

DOI: 10.1039/x0xx00000x

Metalloenzymes naturally achieve various reactivities by assembling of limited types of cofactors with endogenous amino acid residues. Enzymes containing metal porphyrinoid cofactors such as heme, cobalamin and F430 exert precise control over the reactivities of the cofactors with protein matrices. This perspective article focuses on our recent efforts to assemble metal complexes of non-natural porphyrinoids within the protein matrix of myoglobin, an oxygen storage hemoprotein. Engineered myoglobins with the suitable metal complexes as artificial cofactors demonstrate unique reactivities toward C–H bond hydroxylation, olefin cyclopropanation, methyl group transfer and methane generation. In these cases, the protein matrix enhances catalytic activities of the cofactors and permits us to monitor the active intermediates. The present findings indicate that placing artificial cofactors in protein matrices provides a useful strategy for creating artificial metalloenzymes that catalyse otherwise unfavourable reactions and providing enzyme models for elucidating the complicated reaction mechanisms of natural enzymes.

## Introduction

Metalloenzymes catalyse wide range reactions under mild physiological conditions, despite being naturally constructed from limited building resources. Metal ions and metal-containing cofactors must be held within proteins which are generally formed of twenty standard amino acids.<sup>1</sup> The physicochemical properties of metal ions/metal cofactors, which by themselves can be considered as toxic, are regulated by protein matrices to enhance the catalytic activity toward target reactions and to prevent the undesirable side reactions.<sup>2</sup> The metal ions/metal cofactors themselves have inherent reactivity which is significantly regulated by protein matrices to provide specific catalytic activity (Fig. 1a). Amino acid residues in protein matrices support the immobilization of metal ions/cofactors, activation of metal centers, and assistance of substrate access. Among naturally occurring cofactors, metal porphyrinoids are common cofactors, including heme, cobalamin and F430 (Fig. 1b).<sup>3</sup> Heme, a porphyrin iron complex, is one of the most highly studied cofactors.<sup>4</sup> Hemoproteins play important roles in oxygen transport/storage, electron transfer, and catalysis in biological systems.<sup>5</sup> In particular, hemoproteins catalyse various diverse reactions such as monooxygenation,<sup>6</sup> oxidation,<sup>7</sup> H<sub>2</sub>O<sub>2</sub>-dismutation,<sup>8</sup> and oxygen reduction.<sup>9</sup> Cobalamin is a Co complex of corrin, a highly saturated porphyrinoid. Methyl group transfer and 1,2-rearrangement reactions are catalysed by cobalamin-dependent enzymes.<sup>10</sup> F430 is a Ni complex of hydrocorphine, a highly saturated

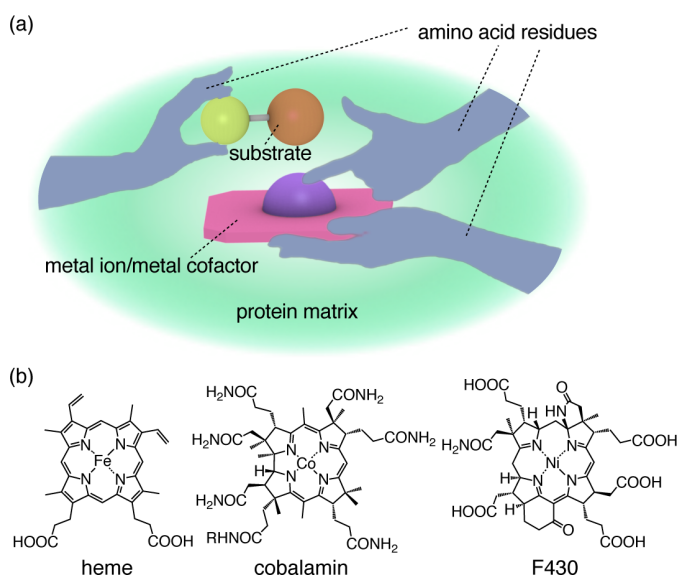


**Fig. 1** (a) Conceptual representation of a metalloenzyme: hands representing amino acids residues play roles in immobilization and activation of a metal ion/metal cofactor as well as supporting binding of a substrate. (b) Molecular structures of metal porphyrinoid cofactors: heme, cobalamin and F430. R in cobalamin represents a side chain including a dimethylbenzimidazole moiety.

porphyrin. This cofactor has unique reactivity in reversibly catalysing conversion of methane to methyl sulphide derivatives in protein matrices under anaerobic conditions.<sup>11</sup> In all cases, the individual enzymes efficiently promote the reactions, while the cofactor by itself is generally ineffective. This indicates that individual protein matrices provide specific control over the reactivities of the cofactors. Inspired by this

Department of Applied Chemistry, Graduate School of Engineering, Osaka University, Suita, 565-0871, Japan. Email: oohora@chem.eng.osaka-u.ac.jp; thayashi@chem.eng.osaka-u.ac.jp

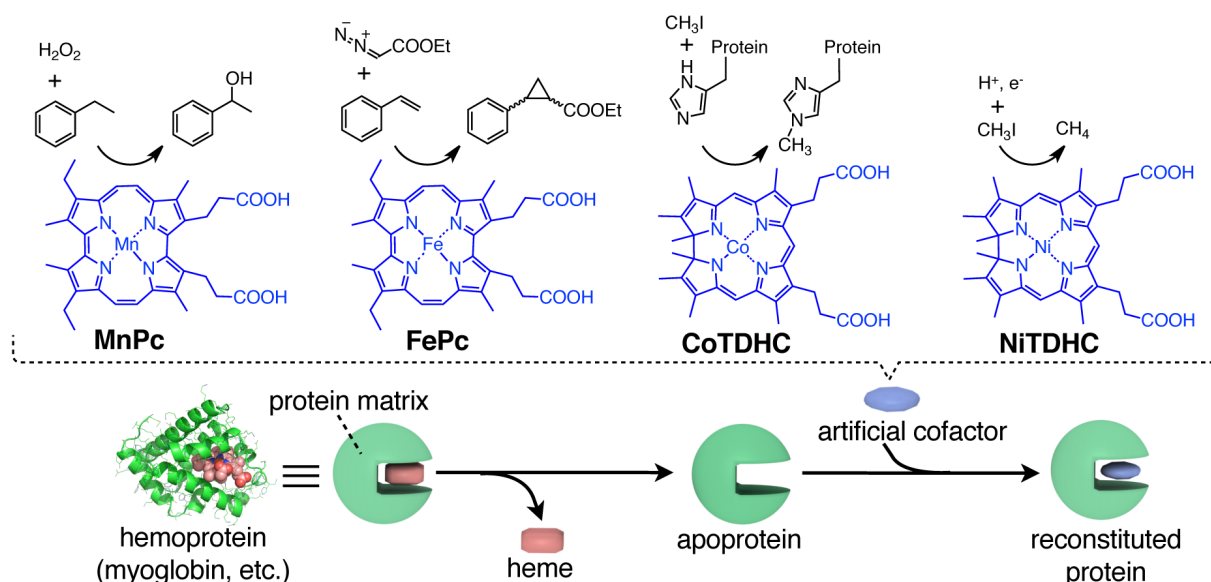


Fig. 2 Schematic representation of hemoprotein reconstitution with artificial cofactors which are highlighted in this article.

concept, protein engineering efforts in the fields of hemoprotein and/or porphyrin chemistry have contributed to the creation of artificial metalloenzymes.<sup>12,13</sup> This perspective article summarizes recent studies to produce the engineered hemoproteins with objective of developing artificial metalloenzymes using biological and synthetic approaches (Fig. 2).

## Engineered hemoproteins toward artificial metalloenzymes

Hemoprotein engineering has been investigated over two decades.<sup>14–16</sup> In this review, we focus on more recent investigations to repurpose hemoproteins toward developments of artificial metalloenzymes.<sup>17</sup> Effort to modify hemoproteins typically involve either mutagenesis or replacement of heme with an artificial cofactor. Mutagenesis is a common technique in protein science and represents a powerful tool for hemoprotein engineering. Here, we think that metalloprotein mutants catalysing non-natural reactions are also regarded as artificial metalloenzymes in a broad sense, although they do not contain artificial metal complexes which are required for artificial metalloenzymes in the narrow definition. For instance, Frances Arnold and co-workers reported that cytochrome P450, a monooxygenase, can be converted to an artificial metalloenzyme capable of catalysing carbene-insertion,<sup>18,19</sup> C–H bond amination,<sup>20,21</sup> and silane oxidation reactions.<sup>22</sup> Directed evolution using random/site-saturated mutations and high throughput screening is an emergent strategy to achieve the activation of inert bonds, and to develop reactions with high selectivity, and high efficiency.<sup>23</sup> This strategy provides an important contribution toward practical use of hemoprotein-based artificial metalloenzymes. Fasan and co-workers demonstrated an enantioselective cyclopropanation reaction of styrene derivatives even using simple hemoprotein, myoglobin (Mb), with suitable

mutations.<sup>24,25</sup> Furthermore, they reported that appropriate Mb mutants show high catalytic activities toward trifluoromethylcarbene transfer reaction,<sup>26</sup> intermolecular carbene S–H insertion reaction,<sup>27</sup> olefination of aldehydes,<sup>28</sup> Doyle-Kirmse reaction,<sup>29</sup> C–H functionalization of unprotected indoles<sup>30</sup> and nitrene transfer reaction.<sup>31</sup> Also, Fasan and co-workers found that cytochrome P450 and Mb mutants catalyse azide-conversion reactions to aldehydes and ketones.<sup>32,33</sup> Lin and co-workers identified a unique mutant of Mb with a covalent cross-linkage of heme and an introduced tyrosine residue and determine that the modification enhances peroxidase activity to extent that it essentially matches that of a native peroxidase enzyme.<sup>34–36</sup> Several recent efforts have involved substitution of amino acid residues with non-canonical amino acid residues.<sup>37–38</sup> Lu, Wang and co-workers have replicated the activity of cytochrome c oxidase using a mutant of Mb with a Cu-binding site which includes a phenol-attached histidine in the heme pocket.<sup>39,40</sup> Hilvert and co-workers have revealed that introduction of an N-methyl histidine as an axial ligand of heme in a hemoprotein enables cyclopropanation of styrene without reductants under aerobic conditions and capture of a carbene–heme adduct within a crystal structure.<sup>33</sup> Green and co-workers constructed a cytochrome P450 mutant with selenocysteine as an axial ligand, enhancing the reactivity of the active intermediate for C–H bond hydroxylation.<sup>42</sup>

Several groups have investigated replacing heme with an artificial metal cofactor to develop artificial metalloenzymes.<sup>43–45</sup> The general scheme is displayed in Fig. 2 and includes removal of heme from a hemoprotein to provide an apoprotein with a space permitting insertion of an artificial cofactor to generate a reconstituted protein. There are three main strategies currently employed in designing an artificial heme cofactor: (i) metal-substitution of heme, (ii) modification of peripheral functional groups of the porphyrin ligand and (iii) providing a non-natural porphyrinoid framework. This section describes the first two strategies and the third strategy is summarized in the next

section. Recent prominent efforts using metal substituted cofactors have been demonstrated by John Hartwig and co-workers, who incorporated an Ir-porphyrin into apoproteins of cytochrome P450 and Mb.<sup>46-48</sup> The reconstituted proteins were found to catalyse enantioselective carbene insertion into alkanes and alkenes. Reconstitution of Mb with metal-substituted heme in development of a carbene insertion catalyst has been also studied by Fasan<sup>49</sup> and Lehnert.<sup>50</sup> In these investigations, Mn, Co, Cu, Ru, and Ir were utilized as the metal centers. Ghirlanda and co-workers reported that Co porphyrin can be used as a cofactor to catalyse hydrogen evolution.<sup>51</sup> Zhang and co-workers demonstrated that Mn-porphyrin has unique oxidation activity in Mb mutants.<sup>52</sup> Recently, Lin and co-workers reported that Mb mutants reconstituted with Zn-porphyrin exhibit photo-induced DNA cleavage activities.<sup>53</sup> In contrast to metal substitution, our group has demonstrated the modification of propionate side chains with dendrons.<sup>54,55</sup> Reconstituted Mb with this modified heme dramatically enhances the peroxidase activity because the dendron functions as a substrate-binding moiety. Flavin-tethered heme was also synthesized to provide a deformylation reaction of 2-phenylpropionaldehyde via reductive activation of oxygen in the protein.<sup>56</sup> Thus, metal substitution and modification of propionate side chains clearly enhances the catalytic activity of hemoproteins.

### Metal complexes of non-natural porphyrinoid/non-porphyrinoid cofactors in protein matrices

Metal complexes of non-natural porphyrinoid frameworks have the potential to provide significantly different reactivities relative to heme because porphyrinoid frameworks with intrinsically different structures provide unique characteristics relative to the natural porphyrin framework.<sup>57-61</sup> Modified corrole frameworks have been among the most highly studied non-natural porphyrinoid frameworks. The corrole frameworks lacks a carbon atom between two of the four pyrrole units, relative to the porphyrin framework.<sup>57-59</sup> In contrast to the dianionic character of porphyrin as a metal ligand, corrole has trianionic character and its metal complexes demonstrate high oxidation reactivity.<sup>57</sup> Gross and co-workers have reported enantioselective sulphoxidation of thioanisole by Fe and Mn complexes of corrole bound within the protein matrix of albumin.<sup>62</sup> Bröring, Frankenberg-Dinkel and co-workers found that Fe corrole has unique reactivity as a substrate in heme oxygenase.<sup>63</sup> Our group has described a Mb reconstituted with Fe corrole which significantly enhances peroxidase activity.<sup>64</sup> Another unique porphyrinoid framework used to construct an artificial metalloprotein is porphycene, a constitutional isomer of porphyrin which has lower symmetry.<sup>60,61,65,66</sup> Our group discovered that Fe porphycene (**FePc**) in Mb has remarkable oxygen-binding affinity as well as peroxidase activity.<sup>67-69</sup> Furthermore, the high-valent species of **FePc** was observed in the protein matrix of horseradish peroxidase and exhibits

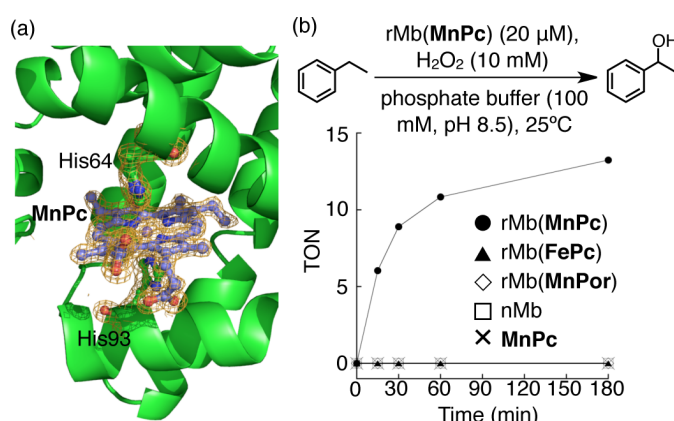


**Fig. 3** (a) Crystal structure of rMb(**MnPc**). (b) Scheme of H<sub>2</sub>O<sub>2</sub>-dependent ethylbenzene hydroxylation and time course plots of TON for this reaction. Reprinted with permission from ref. 72. Copyright (2013) American Chemical Society.

greater oxidation activity.<sup>70</sup> Additional studies of **FePc** and Mn porphycene (**MnPc**) in context of developing hydroxylation and cyclopropanation, respectively, in the protein matrix of Mb are described in the following sections.<sup>71-73</sup> Although metal complexes of other porphyrinoids such as hemiporphycene,<sup>74</sup> oxaporphyrin,<sup>75</sup> azaporphyrin<sup>76</sup> and phthalocyanine<sup>77</sup> has also been employed as artificial cofactors of artificial metalloproteins, development of catalysts using these metal cofactors has been quite limited with the exception of the Diels-Alder reaction catalysed by copper phthalocyanine in albumin.<sup>78</sup>

Several metal complexes including a Schiff-base such as salen have been incorporated into hemoprotein matrices, although these molecules are not considered to be porphyrinoids.<sup>79</sup> Ueno, Watanabe and co-workers reported the crystal structures of several artificial metalloproteins, where Fe ligated to a Schiff-base ligand was found to promote rapid NADH and O<sub>2</sub> consumption in heme oxygenase.<sup>80</sup> Lu and co-workers demonstrated the covalently attached Mn salen complex in the heme-binding site of Mb, catalysing enantioselective sulphoxidation.<sup>81</sup> Artero revealed that insertion of cobaloxime, a cobalt complex of Schiff-base ligands, into apoprotein of Mb provides an artificial hydrogenase.<sup>82</sup> Thus, metal complexes of non-natural porphyrinoids and non-porphyrinoid ligand have been broadly investigated as artificial cofactors of artificial metalloenzymes.

### C–H bond hydroxylation by myoglobin reconstituted with manganese porphycene

Several cytochrome P450s catalyse C–H bond hydroxylation, whereas native Mb (nMb) does not show such catalytic activity despite including same cofactor.<sup>83-85</sup> Although the several investigations have attempted to enhance oxidation activity of Mb by engineering specific mutations, outer substrate monooxygenation of C–H bond has not been achieved.<sup>15</sup> Our group identified several artificial cofactors including Fe as a metal center in attempts to improve peroxidase activity of Mb but C–H bond hydroxylation was not demonstrated. In this

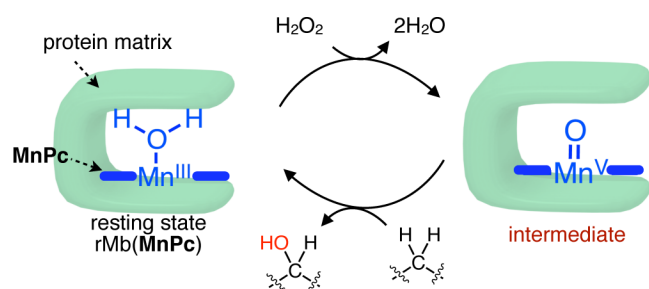


**Fig. 4** Proposed catalytic cycle of  $\text{H}_2\text{O}_2$ -dependent C–H bond hydroxylation by  $\text{rMb}(\text{MnPc})$ . Reprinted with permission from ref. 73. Copyright (2017) American Chemical Society.

context, an artificial cofactor with Mn was investigated because several research groups had demonstrated that Mn complexes have the potential to activate the C–H bond with a high valent-oxo intermediate.<sup>86–90</sup> According to this concept, **MnPc** was designed as an artificial cofactor (Fig. 2).<sup>72,73</sup> Although Mb reconstituted with Mn porphyrin (**MnPc**) was reported to show moderate peroxidase activity, the porphycene framework was expected to provide higher activity to its Mn complex because the results of our previous study had indicated that Fe porphycene in horseradish peroxidase has higher activity relative to the native protein.<sup>70</sup> **MnPc** was successfully inserted into Mb to construct  $\text{rMb}(\text{MnPc})$ , which was characterized by UV-vis spectroscopy, mass spectrometry and X-ray crystal structure analysis. The crystal structure is shown in Fig. 3a, revealing axial coordination to the Mn center by His93, an axial ligand of heme in nMb. Superimposed structures indicate no clear differences in the main chains of the proteins between  $\text{rMb}(\text{MnPc})$  and nMb. In the presence of hydrogen peroxide and ethylbenzene as an oxidant and substrate, respectively,  $\text{rMb}(\text{MnPc})$  provides 1-phenylethanol without any side products such as ketones. The turnover number (TON) depends on pH and attain a value reached of 13 at pH 8.5. Interestingly, the other Mbs containing heme, **FePc**, **MnPc** do not yield any products (Fig. 3b). Furthermore, **MnPc** without the protein matrix does not promote catalysis, indicating that the Mb matrix provides a suitable reaction field to **MnPc** to promote C–H bond hydroxylation. When the deuterated ethylbenzene was employed as a substrate, a kinetic isotope effect was observed, indicating a decrease in the reaction rate relative to the normal substrate.  $\text{rMb}(\text{MnPc})$  catalyses the hydroxylation of toluene and cyclohexane and logarithm plots of the rate constants for  $\text{rMb}$ -catalysed hydroxylation of ethylbenzene, toluene and cyclohexane against bond dissociation energy show a linear relationship with a negative slope. These findings indicate that the C–H bond activation is one of the rate-limiting steps in this catalysis. The reaction was performed with  $^{18}\text{O}$ -labeled hydrogen peroxide and the  $^{18}\text{O}$ -introduced product was obtained quantitatively. This result indicates that the OH-rebound process is followed after the C–H activation. Thus, the C–H bond hydroxylation mechanism of  $\text{rMb}(\text{MnPc})$  is similar to that of cytochrome P450.<sup>83–85</sup>

The details of the reaction were investigated, and the proposed mechanism is shown in Fig. 4. The reaction of  $\text{rMb}$

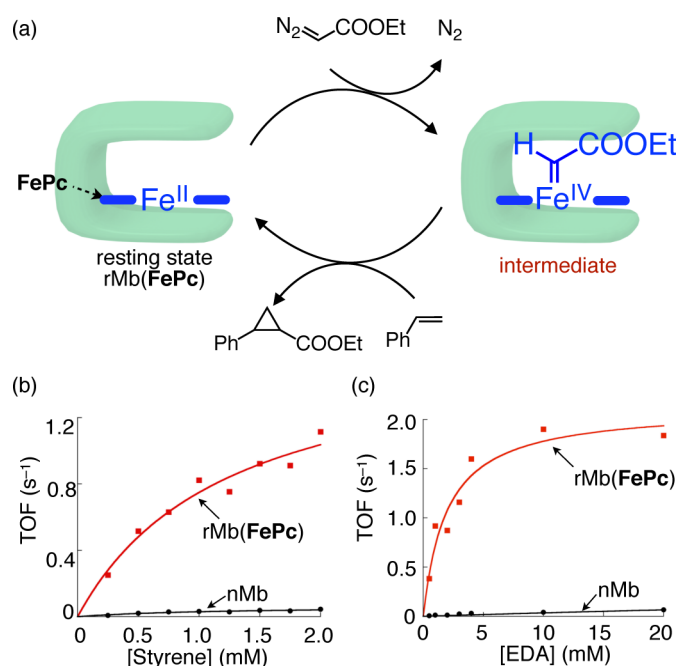


**Fig. 5** (a) Proposed catalytic cycle of cyclopropanation of styrene by  $\text{rMb}(\text{FePc})$ . (b,c) Plots of TOF for the cyclopropanation against various concentration of styrene (b) and EDA (c). The plots are fitted to the conventional Michaelis-Menten equation. Reprinted with permission from ref. 71. Copyright (2017) American Chemical Society.

with *meta*-chloroperoxybenzoic acid (mCPBA) was monitored to determine transient UV-vis spectral changes using stopped flow techniques. Within two seconds of mixing, a UV-vis spectrum indicating a new species was observed. This generated species was tentatively regarded as the intermediate in catalysis. This species was characterized by freeze quenched EPR with perpendicular and parallel modes, which are active for half integer and integer spins, respectively. Before mixing with peracid, we observed broad signals in the perpendicular mode, whereas sharp signals split by nuclear spin were observed in the parallel mode. This result indicates that the resting state of  $\text{rMb}(\text{MnPc})$  is a Mn(III) species. After mixing with peracid, no signals were observed in both modes of EPR. The Mn(IV) porphyrinoid species has been reported to be  $S = 3/2$  with strong signals in perpendicular mode EPR. Thus, it was determined that the reaction of  $\text{rMb}(\text{MnPc})$  with peracid forms the low spin Mn(V) intermediate ( $S = 0$ ) as an EPR-silent species. The obtained intermediate was reacted with ethylbenzene sulphonate as a substrate to provide the resting state of  $\text{rMb}(\text{MnPc})$  and hydroxidized products in double mixing stopped flow techniques, also indicating that the observed intermediate should be an active species. The UV-vis spectral changes observed under the conditions of various substrate concentrations provide apparent second order rate constants:  $k_2$ . These constants depend on substrates and the logarithm plots of  $k_2$  values against bond dissociation energy provide a linear relationship with a negative slope. The slope is identical to the slope derived from similar plots of rate constants for product formation in catalysis. This finding provides strong support for the proposal that the C–H bond activation is a rate-determining step in catalysis. These investigations of **MnPc**



provide the first demonstration of the C–H bond hydroxylation in outer substrates using the native protein matrix of Mb. The detectable intermediate of **MnPc** will advance our understanding of this class of catalytic activity.

### Cyclopropanation of styrene by myoglobin reconstituted with iron porphyrine

Hemoproteins has been considered as useful catalysts for cyclopropanation of olefins via metallocarbene species. Several mutants of cytochrome P450 and Mb have demonstrated the high TON and enantioselectivity.<sup>24,25,41,91,92</sup> Reconstituted hemoproteins with metal-substituted heme have also been investigated in this area.<sup>38-42</sup> However, investigations of cyclopropanation by artificial cofactors with non-natural porphyrinoid frameworks have been rare.<sup>93,94</sup> In this context, our group focused on **FePc** which have very different physicochemical properties relative to heme in a protein matrix.<sup>67-70</sup> First, the catalytic activity of reconstituted Mb with **FePc** (rMb(**FePc**)) for the reaction of styrene with ethyl diazoacetate (EDA) was evaluated in the presence of dithionite.<sup>71</sup> Fig. 5a shows a plausible catalytic cycle. Interestingly, rMb(**FePc**) has a 35-fold higher turnover frequency (TOF) for cyclopropanation than nMb. Next, detailed Michaelis–Menten parameters were determined (Fig. 5bc). Under conditions using various concentrations of styrene and a large excess of EDA (10 mM),  $k_{\text{cat}}$  of rMb(**FePc**) is 26-fold higher than that of nMb. In contrast,  $K_{\text{m}}$  of rMb(**FePc**) is mostly consistent with that of nMb. Under conditions using various concentrations of EDA and a large excess of styrene (2.0 mM), nMb does not demonstrate conventional saturation of TOF in the plots, indicating that the concentration of EDA limits the rate of the cyclopropanation reaction. In the case of rMb(**FePc**), saturation was clearly observed with  $k_{\text{cat}}$  and  $K_{\text{m}}$  values of  $2.1 \text{ s}^{-1}$  and 1.9 mM, respectively. This  $k_{\text{cat}}$  value is essentially identical to the value derived from the experiment performed using the various concentrations of styrene, suggesting that the mechanism of cyclopropanation catalysed by rMb(**FePc**) can be elucidated via steady state experiments.

Evaluation of catalytic activity indicates that the reactivities of rMb(**FePc**) and nMb with EDA are different. Thus, the reaction of the protein with EDA was evaluated by transient UV-vis spectral changes using stopped flow techniques. The reaction of rMb(**FePc**) with EDA rapidly generates the new species within 0.5 s. This species was further confirmed to be reactive with styrene, providing the cyclopropane derivative and the resting state in a reaction monitored using the double mixing stopped flow method. This result shows that the monitored species is an active metallocarbene species. This is first spectroscopic observation of a reactive metallocarbene species in a hemoprotein. Related research has resulted in direct characterization of the metallocarbene species in a crystal structure of a hemoprotein shortly afterward.<sup>41,95</sup> Although the reaction of nMb with EDA also provides spectral

changes indicating formation of a new species with a slower reaction rate than that of rMb(**FePc**), this species does not react with styrene. The monitored species for nMb is believed to be an inactive species such as N-alkylated heme. The reaction of nMb with EDA is 615-times slower than the same reaction catalysed by rMb(**FePc**). The high reactivity of rMb(**FePc**) for EDA provides efficient cyclopropanation catalysis.

The difference in reactivity was elucidated by theoretical studies. DFT calculations were performed at the B97D/6-31g\* level to estimate the potential energy for the reaction of the imidazole-ligated cofactors with EDA to form metallocarbene species. The key difference between heme and **FePc** is found in their spin states in the resting states in contrast to those of the metallocarbene species. Spin states of the resting states of heme and **FePc** are quintet (high spin) and triplet (intermediate spin), respectively. However, both of the metallocarbene species are estimated to be singlet. Thus, **FePc** requires only one intersystem crossing event to form a metallocarbene intermediate in contrast to two intersystem crossings being required for heme. The related energy barriers result in very different reaction rates between rMb(**FePc**) and nMb. These results of investigations of artificial cofactors will contribute to the development of useful artificial metalloenzymes as carbene insertion catalysts.

### A model of methionine synthase by myoglobin reconstituted with cobalt tetradehydrocorrin

Cobalamin-dependent methionine synthase catalyses methyl group transfer reaction from *N*-methyl tetrahydrofolate to homocysteine, providing methionine and tetrahydrofolate.<sup>10,96-101</sup> Although several studies using this enzyme have been reported, its detailed mechanism has not been elucidated completely due to the complicated structure of cobalamin as a cofactor and the large protein matrix of the enzyme. These efforts suggest that the reaction of a Co(I) species with *N*-methyl tetrahydrofolate forms a methylated Co(III) species, followed by the reaction with homocysteine to afford methionine and the Co(I) species. Among the reaction intermediates, the crystal structure of the Co(I) species has not been determined and the activation mechanism of the methylated Co(III) species has not been elucidated completely because methyl cobalamin itself is relatively unreactive.<sup>102,103</sup> In this context, we considered that a

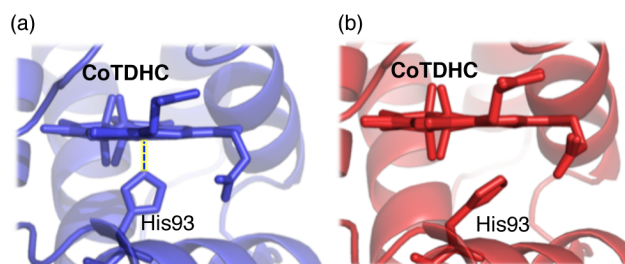


**Fig. 6** (a) Crystal structure of Co(II) species of rMb(**CoTDHC**). (b) Crystal structure of Co(I) species of rMb(**CoTDHC**), which was prepared by soaking of the crystal of the Co(II) species into dithionite solution. Reproduced with permission from ref. 104. Copyright (2014) The Royal Society of Chemistry.

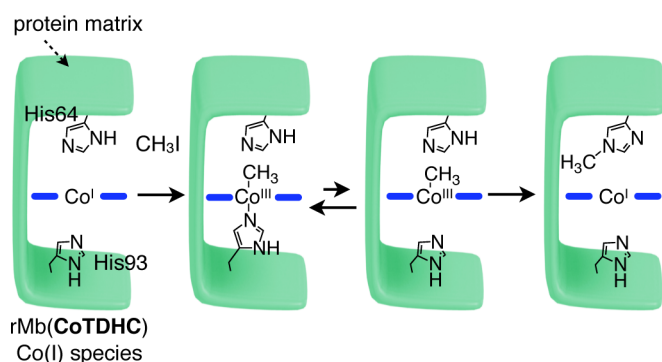


**Fig. 7** Proposed mechanism of intra-protein methyl group transfer in rMb(CoTDHC).

suitable protein-based model system using a simple cofactor and protein matrix would provide significant information. Thus, Co tetrahydrocorrin and apo-Mb were employed as a simple cofactor and protein matrix (Fig. 2).<sup>104-108</sup> Several investigations of Co tetrahydrocorrin derivatives in organic solvents were reported by Dolphin as model studies of cobalamin, indicating that the TDHC ligand stabilizes the low valent species of the metal center, whereas the methylated species is unavailable due to the low reactivity of the Co(I) species.<sup>109,110</sup>

Co tetrahydrocorrin with two propionate side chains (CoTDHC) was designed, synthesized and inserted into the protein matrix of Mb. The reconstituted Mb with CoTDHC (rMb(CoTDHC)) was characterized by UV-vis spectroscopy and ESI MS. Under ambient conditions, its EPR spectrum reveals that this rMb contains a Co(II) species. Typical hyperfine splitting coupled by the nuclear spin of Co(II) and superhyperfine splitting by an axially ligated nitrogen atom were observed. The crystal structure of rMb(CoTDHC) also indicates that His93 is axially coordinated to the Co(II) center in the overall maintained protein structure (Fig. 6a). The crystal of rMb was soaked in an aqueous solution of dithionite, causing a colour change which indicates formation of the Co(I) species. Surprisingly, this crystal provided an atomic-scale structure of rMb(CoTDHC) with the Co(I) species. In the structure, the coordinated His93 is flipped and Co(I) has a tetracoordinated structure (Fig. 6b). This is the first demonstration of a crystal structure of a tetracoordinated Co(I) corrinoid species. This solution state Co(I) species was also characterized by UV-vis and EPR spectra. Thus, the tetracoordinated structure of the Co(I) species has been directly clarified as an analogue of the important intermediate suggested to exist during catalysis by methionine synthase.

An additional reaction of the Co(I) species in rMb(CoTDHC) with methyl iodide was investigated. Although the reported CoTDHC derivatives in organic solvents do not form the methylated species, rMb(CoTDHC) yields the methylated Co(III) species which was characterized by UV-vis, EPR and mass spectra. Redox potential measurements and DFT calculations support the speculation that the more positively shifted Co(III)/Co(II) redox couple provides a more stable methylated Co(III) species. Furthermore, it was found that the methyl group

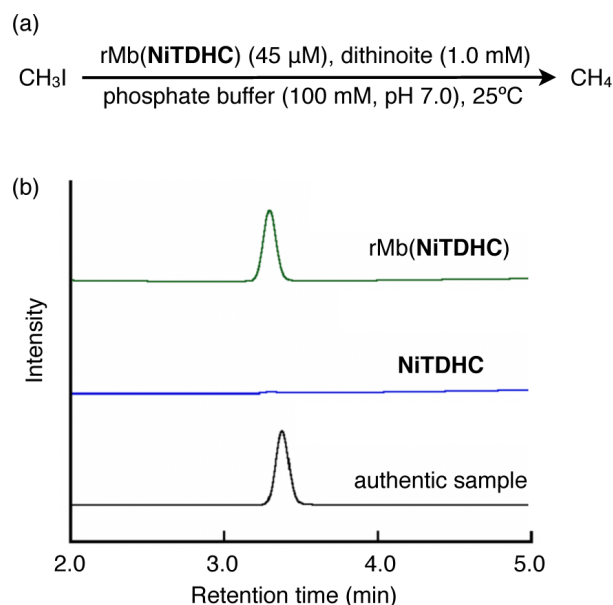


**Fig. 8** (a) Scheme of methane generation promoted by rMb(NiTDHC). (b) GC traces for a methane-generating reaction promoted by rMb(NiTDHC) (top) and NiTDHC (middle). A GC trace of an authentic sample of methane gas is displayed at the bottom. Reproduced with permission from ref. 120. Copyright (2019) Wiley-VCH Verlag GmbH & Co. KGaA, Weinheim.

of the Co(III) species is transferred to His64, which is located on the distal side of heme-binding site of the Mb matrix. A peptide including methylated His64 obtained by digestion was characterized by mass and NMR spectra. This indicated that the methyl transfer reaction of methionine synthase was replicated by our simple model system. The intra-protein methyl group transfer in rMb(CoTDHC) was elucidated by the DFT calculation. In the reaction event, we proposed two types of reaction pathways: (i) a one-step pathway with the methyl group transfer occurring by simultaneous de-ligation of histidine, and (ii) a two-step transfer with histidine de-ligation before methyl group transfer. DFT calculations support the latter two-step pathway because de-ligation of the axial ligand does not have a significant energy barrier. Thus, transient de-ligation of the axially coordinated histidine activates the methylated Co(III) species for methyl group transfer (Fig. 7). This finding contributes to the elucidation of the mechanism for the methyl group transfer in methionine synthase.

### A model of methyl coenzyme M reductase by myoglobin reconstituted with nickel tetrahydrocorrin

Methyl coenzyme M reductase (MCR) which contains the F430 cofactor catalyses methane generation in methanogenic archaea.<sup>11,111-114</sup> This enzyme produces methane and a disulphide compound from methyl coenzyme M and coenzyme B. According to several reports, the Ni(I) species of F430 is a key intermediate in the catalysis of MCR, while the mechanism of methane formation from two substrates has not been conclusively established. Two plausible mechanisms have been

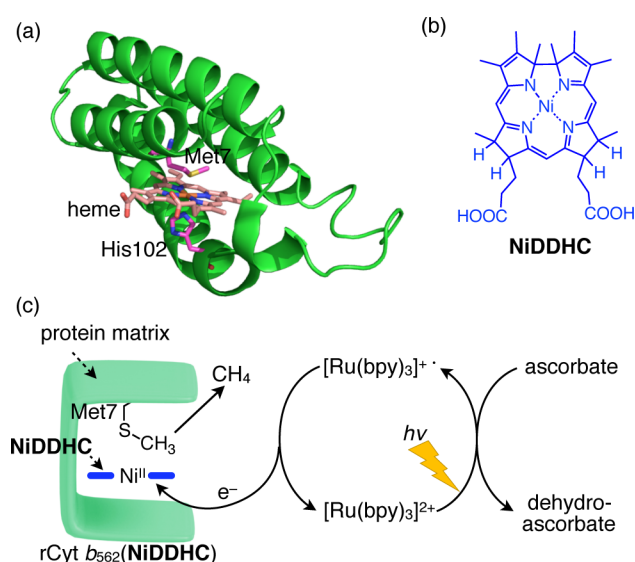


**Fig. 9** (a) Crystal structure of Cyt  $b_{562}$ . (b) Molecular structure of **NiDDHC**. (c) Schematic representation of intra-protein C-S bond cleavage in rCyt  $b_{562}$ (**NiDDHC**) by photo-induced reduction.

proposed: (i) a pathway via the formation of methylated Ni(III) species and (ii) a pathway involving methyl radical species. The complicated structure of the enzyme provides the significant difficulties in revealing important details. Unfortunately, the studies of the model systems have been limited and protein-based models had not been previously investigated.<sup>115-119</sup> In this context, we designed a reconstituted Mb with Ni tetradehydrocorrins as a protein-based model of MCR because this ligand is known to stabilize the low valent metal center.<sup>120,121</sup> We prepared the Ni tetradehydrocorrins with two propionate-side chains (**NiTDHC**) and obtained EPR measurements which revealed that dithionite reduces the Ni(II) species of **NiTDHC** to provide the Ni(I) species in an aqueous solution. In contrast to **NiTDHC**, F430 without the protein matrix and the other model complexes require stronger reductants such as Ti citrate and NaHg to form the Ni(I) state.<sup>115-119</sup> Thus, this highly positive redox potential for the Ni(I)/Ni(II) couple ( $-0.34$  V vs SHE) relative to that of F430 ( $-0.65$  V vs SHE)<sup>122</sup> provides a useful protein-based MCR model. Next, this complex was inserted into apo-Mb to afford rMb(**NiTDHC**). Unfortunately, a crystal structure of rMb(**NiTDHC**) could not be obtained due to the low binding constant of **NiTDHC** for the protein. However, the formation of rMb(**NiTDHC**) was confirmed by UV-vis, CD and mass spectra. In the presence of excess dithionite as a reductant, methane generation from methyl iodide as a methyl source was found to be promoted by rMb(**NiTDHC**) (Fig. 8). Interestingly, only **NiTDHC** does not provide methane gas under the same conditions, indicating that the protein matrix contributes to enhancement of the reactivity of the Ni(I) species. This enhancement was proposed to arise from the negatively shifted redox changes induced by the binding of the cofactor into the protein matrix. This reconstituted protein is the first example of a protein-based model of MCR.

The reconstituted **NiTDHC** hemoprotein system was expanded to cytochrome  $b_{562}$  (Cyt  $b_{562}$ ), a simple electron transfer hemoprotein. Cyt  $b_{562}$  has a bis-coordinated structure with methionine and histidine (Fig. 9a).<sup>123</sup> We considered that the heme binding site of Cyt  $b_{562}$  could mimic the substrate bound form of the active site of MCR, in which methionine, with its C-S group functions as an intra-protein substrate. According to this concept, we prepared the reconstituted Cyt  $b_{562}$  with **NiTDHC**.<sup>124</sup> However, only a negligible amount of methane generation was observed, indicating that the reactivity of the Ni(I) species is insufficient. Reconstitution with Ni didehydrocorrins with two propionate side chains (**NiDDHC**) was attempted because the Co didehydrocorrins has the more negatively shifted redox couples relative to **CoTDHC**.<sup>108</sup> Cyt  $b_{562}$  reconstituted with **NiDDHC** (rCyt  $b_{562}$ (**NiDDHC**)) was found to generate methane under photoreduction conditions with a Ru trisbipyridine complex (Fig. 9). Surprisingly, this reaction was found to occur with cleavage of the methionine residue in the heme-binding site, as validated by mass spectra of the protein matrix after the reaction and a mutation experiment. Further mutation to introduce a cysteine residue as another substrate mimicking coenzyme B in MCR was demonstrated to generate 1.2-times more methane gas relative to the reconstituted protein without the mutation. These results indicate that a suitable arrangement of substrate and redox potential of the Ni center is critical for catalysis by MCR. The system investigated in this work represents the first demonstration of methane formation via intra-protein C-S bond cleavage. Additional detailed investigations of model systems will contribute to elucidation of the mechanism of MCR and development of artificial metalloenzymes related to this reaction.

## Conclusions

Several emergent efforts to convert the hemoproteins into artificial metalloenzymes using artificial cofactors have been recently reported. Similar strategies have been extended to non-porphyrinoid metal complexes in other potent host proteins with reaction sites.<sup>125-130</sup> The artificial metalloenzymes demonstrate unique catalytic reactions with high efficiency, enantioselectivity and chemoselectivity, which trend to be predominantly influenced by the protein matrix. Common characteristics of our artificial cofactors are the unique reactivities generated by the binding into the protein matrix. The hydrophobic heme-binding site with an axial ligand serves as a suitable reaction scaffold to regulate reactivity as well as to enable observation of intermediates. The protein matrix modulates the redox potentials of artificial cofactors and also prevents undesirable side reactions. Generally, evaluation of intermediates of native enzymes is difficult and requires specialized techniques because of substrate specificity and rapid catalytic cycles. Observations of reactive intermediates in the present artificial metalloproteins provide further inspiration in efforts to design of next-generation artificial cofactors and protein matrices to advance this field. Artificial metalloenzymes have great potential to overcome thermodynamic and/or



kinetic stereoselectivity, regioselectivity and chemoselectivity and these selectivities cannot be achieved by small molecular catalysts without specific reaction scaffolds. The precise control of cofactors will contribute to the creation of powerful catalysts.

### Conflicts of interest

There are no conflicts to declare.

### Acknowledgements

We thank for our co-workers including graduate students who contributed to the results shown in this article as well as our collaborators named in the references cited. We gratefully appreciate support from Grants-in-Aid for Scientific Research provided by JSPS KAKENHI Grant Numbers JP15H05804, JP18K19099, JP18KK0156, JP20H02755, JP20H00403 and JST PRESTO (JPMJPR15S2).

### Notes and references

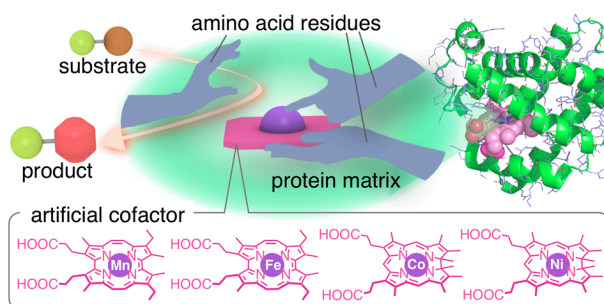
- 1 C. Andreini, I. Bertini, G. Cavallaro, G. L. Holliday and J. M. Thornton, *J. Biol. Inorg. Chem.*, 2008, **13**, 1205.
- 2 Y. Lu, N. Yeung, N. Sieracki and N. M. Marshall, *Nature*, 2009, **460**, 855.
- 3 D. A. Bryant, C. N. Hunter and M. J. Warren, *J. Biol. Chem.*, 2020, **295**, 6888.
- 4 T. L. Poulos, *Chem. Rev.*, 2014, **114**, 3919.
- 5 K. D. Karlin, *Science*, 1993, **261**, 701.
- 6 J. H. Dawson, *Science*, 1988, **249**, 433.
- 7 H. Pelletier and J. Kraut, *Science*, 1992, **258**, 1748.
- 8 I. Fridovich, *Science*, 1978, **201**, 4359.
- 9 T. Tsukihara, H. Aoyama, E. Yamashita, T. Tomizaki, H. Yamaguchi, K. Shinzawa-Itoh, R. Nakashima, R. Yaono and S. Yoshikawa, *Science*, 1996, **272**, 1136.
- 10 B. Kräutler, in *Metal Ions in Life Science*, ed. A. Sigel, H. Sigel and R. K. O. Sigel, Royal Society of Chemistry, Cambridge, 2009, ch. 1, vol. 6, pp. 1–51.
- 11 R. K. Thauer, *Biochemistry*, 2019, **58**, 5198.
- 12 T. Hayashi and K. Oohora, in *Dioxygen-dependent Heme Enzymes*, ed. M. Ikeda-Saito and E. Raven, Royal Society of Chemistry, Cambridge, 2019, pp. 63–78.
- 13 K. Oohora, A. Onoda and T. Hayashi, *Acc. Chem. Res.*, 2019, **52**, 945.
- 14 T. Hayashi and Y. Hisaeda, *Acc. Chem. Res.*, 2002, **35**, 35.
- 15 S. Ozaki, M. P. Roach, T. Matsui and Y. Watanabe, *Acc. Chem. Res.*, 2001, **34**, 818.
- 16 Y. Liu, S. M. Berry and T. D. Pfister, *Chem. Rev.*, 2001, **101**, 3047.
- 17 C. A. Denard, H. Ren and H. Zhao, *Curr. Opin. Chem. Biol.*, 2015, **25**, 55.
- 18 R. K. Zhang, K. Chen, X. Huang, L. Wohlschlagler, H. Renata and F. H. Arnold, *Nature*, 2019, **565**, 67.
- 19 R. K. Zhang, X. Huang and F. H. Arnold, *Curr. Opin. Chem. Biol.*, 2019, **49**, 67.
- 20 C. K. Prier, R. K. Zhang, A. R. Buller, S. Brinkmann-Chen and F. H. Arnold, *Nat. Chem.*, 2017, **9**, 629.
- 21 Z. J. Jia, S. Gao and F. H. Arnold, *J. Am. Chem. Soc.*, 2020, **142**, 10279.
- 22 S. Bähr, S. Brinkmann-Chen, M. Garcia-Borràs, J. M. Roberts, D. E. Katsoulis, K. N. Houk and F. H. Arnold, *Angew. Chem. Int. Ed.*, 2020, **59**, 15507.
- 23 S. C. Hammer, G. Kubik, E. Watkins, S. Huang, H. Minges and F. H. Arnold, *Science*, 2017, **358**, 215.
- 24 M. Bordeaux, V. Tyagi and R. Fasan, *Angew. Chem. Int. Ed.*, 2015, **54**, 1744.
- 25 P. Bajaj, G. Sreenilayam, V. Tyagi and R. Fasan, *Angew. Chem. Int. Ed.*, 2016, **55**, 16110.
- 26 A. Tinoco, V. Steck, V. Tyagi and R. Fasan, *J. Am. Chem. Soc.*, 2017, **139**, 5293.
- 27 V. Tyagi, R. B. Bonn and R. Fasan, *Chem. Sci.*, 2015, **6**, 2488.
- 28 V. Tyagi and R. Fasan, *Angew. Chem., Int. Ed.*, 2016, **55**, 2512.
- 29 V. Tyagi, G. Sreenilayam, P. Bajaj, A. Tinoco and R. Fasan, *Angew. Chem., Int. Ed.*, 2016, **55**, 13562.
- 30 D. A. Vargas, A. Tinoco, V. Tyagi and R. Fasan, *Angew. Chem., Int. Ed.*, 2018, **57**, 9911.
- 31 M. Bordeaux, R. Singh and R. Fasan, *Bioorg. Med. Chem.*, 2014, **22**, 5697.
- 32 S. Giovani, R. Singh and R. Fasan, *Chem. Sci.*, 2016, **7**, 234.
- 33 S. Giovani, H. Alwaseem and R. Fasan, *ChemCatChem*, 2016, **8**, 2609.
- 34 F. Liao, J.-K. Xu, J. Luo, S.-Q. Gao, X.-J. Wang and Y.-W. Lin, *Dalton Trans.*, 2020, **49**, 5029.
- 35 P. Zhang, H. Yuan, J. Xu, X.-J. Wang, S.-Q. Gao, Xi. Tan and Y.-W. Lin, *ACS Catal.*, 2020, **10**, 891.
- 36 C. Liu, H. Yuan, F. Liao, C.-W. Wei, K.-J. Du, S.-Q. Gao, X. Tan and Y.-W. Lin, *Chem. Commun.*, 2019, **55**, 6610.
- 37 I. Drienovská and G. Roelfes, *Nat. Catal.*, 2020, **3**, 192.
- 38 J. Zhao, A. J. Burke and A. P. Green, *Curr. Opin. Chem. Biol.*, 2020, **55**, 136.
- 39 X. Liu, Y. Yu, C. Hu, W. Zhang, Y. Lu and J. Wang, *Angew. Chem. Int. Ed.*, 2012, **51**, 4312.
- 40 Y. Yu, X. Lv, J. Li, Q. Zhou, C. Cui, P. Hosseinzadeh, A. Mukherjee, M. J. Nilges, J. Wang and Y. Lu, *J. Am. Chem. Soc.*, 2015, **137**, 4594.
- 41 T. Hayashi, M. Tinzl, T. Mori, U. Kregel, J. Proppe, J. Soetbeer, D. Klose, G. Jeschke, M. Reiher and D. Hilvert, *Nat. Catal.*, 2018, **1**, 578.
- 42 E. L. Onderko, A. Silakov, T. H. Yosca and M. T. Green, *Nat. Chem.*, 2017, **9**, 623.
- 43 T. Hayashi, in *Coordination Chemistry in Protein Cages*, ed. T. Ueno and Y. Watanabe, John Wiley & Sons, Hoboken, New Jersey, 2013, pp. 87–110.
- 44 T. Hayashi, in *Handbook of Porphyrin Sciences*, ed. K.M. Kadish, K.M. Smith and R. Guilard, Vol. 5, World Scientific, Singapore, 2010, pp. 1–67.
- 45 K. Oohora and T. Hayashi, *Methods Enzymol.*, 2016, **580**, 439.
- 46 S. N. Natoli and J. F. Hartwig, *Acc. Chem. Res.*, 2019, **52**, 326.
- 47 P. Dydio, H. M. Key, A. Nazarenko, J. Y.-E. Rha, V. Seyedkazemi, D. S. Clark and J. F. Hartwig, *Science*, 2016, **354**, 102.
- 48 H. M. Key, P. Dydio, D. S. Clark and J. F. Hartwig, *Nature*, 2016, **534**, 534.
- 49 G. Sreenilayam, E. J. Moore, V. Steck and R. Fasan, *Adv. Synth. Catal.*, 2017, **359**, 2076.
- 50 M. W. Wolf, D. A. Vargas, and N. Lehnert, *Inorg. Chem.*, 2017, **56**, 5623.
- 51 D. J. Sommer, M. D. Vaughn and G. Ghirlanda, *Chem. Commun.*, 2014, **50**, 15852.
- 52 Y.-B. Cai, X.-H. Li, J. Jing and J.-L. Zhang, *Metallomics*, 2013, **5**, 828.
- 53 Z.-H. Shi, K.-J. Du, B. He, S.-Q. Gao, G.-B. Wen and Y.-W. Lin, *Inorg. Chem. Front.*, 2017, **4**, 2033.
- 54 H. Sato, T. Hayashi, T. Ando, Y. Hisaeda, T. Ueno and Y. Watanabe, *J. Am. Chem. Soc.*, 2004, **126**, 436.
- 55 T. Matsuo, K. Fukumoto, T. Watanabe and T. Hayashi, *Chem. Asian J.*, 2011, **6**, 2491.
- 56 T. Matsuo, T. Hayashi and Y. Hisaeda, *J. Am. Chem. Soc.*, 2002, **124**, 11234.
- 57 R. A. Baglia, J. P. T. Zaragoza and D. P. Goldberg, *Chem. Rev.*, 2017, **117**, 13320.

- 58 R. Orłowski, D. Gryko and D. T. Gryko, *Chem. Rev.*, 2017, **117**, 3102.
- 59 Y. Fang, Z. Ou and K. M. Kadish, *Chem. Rev.*, 2017, **117**, 3377.
- 60 J. Waluk, *Chem. Rev.*, 2017, **117**, 2447.
- 61 G. Anguera and D. Sánchez-García, *Chem. Rev.*, 2017, **117**, 2481.
- 62 A. Mahammed and Z. Gross, *J. Am. Chem. Soc.*, 2005, **127**, 2883.
- 63 B. Gisk, F. Brégier, R. A. Krüger, M. Bröring and N. Frankenberg-Dinke, *Biochemistry*, 2010, **49**, 10042.
- 64 T. Matsuo, A. Hayashi, M. Abe, T. Matsuda, Y. Hisaeda and T. Hayashi, *J. Am. Chem. Soc.*, 2009, **131**, 15124.
- 65 E. Vogel, M. Köcher, H. Schmickler and J. Lex, *Angew. Chem. Int. Ed.*, 1986, **25**, 257.
- 66 K. Oohora, A. Ogawa, T. Fukuda, A. Onoda, J.-Y. Hasegawa and T. Hayashi, *Angew. Chem. Int. Ed.*, 2015, **54**, 6227.
- 67 T. Hayashi, H. Dejima, T. Matsuo, H. Sato, D. Murata and Y. Hisaeda, *J. Am. Chem. Soc.*, 2002, **124**, 11226.
- 68 T. Matsuo, H. Dejima, S. Hirota, D. Murata, H. Sato, T. Ikegami, H. Hori, Y. Hisaeda and T. Hayashi, *J. Am. Chem. Soc.*, 2004, **126**, 16007.
- 69 T. Hayashi, D. Murata, M. Makino, H. Sugimoto, T. Matsuo, H. Sato, Y. Shiro and Y. Hisaeda, *Inorg. Chem.*, 2006, **45**, 10530.
- 70 T. Matsuo, D. Murata, Y. Hisaeda, H. Hori and T. Hayashi, *J. Am. Chem. Soc.*, 2007, **129**, 12906.
- 71 K. Oohora, H. Meichin, L. Zhao, M. W. Wolf, A. Nakayama, J. Hasegawa, N. Lehnert and T. Hayashi, *J. Am. Chem. Soc.*, 2017, **139**, 17265.
- 72 K. Oohora, Y. Kihira, E. Mizohata, T. Inoue and T. Hayashi, *J. Am. Chem. Soc.*, 2013, **135**, 17282.
- 73 K. Oohora, H. Meichin, Y. Kihira, H. Sugimoto, Y. Shiro and T. Hayashi, *J. Am. Chem. Soc.*, 2017, **139**, 18460.
- 74 S. Neya, K. Imai, H. Hori, H. Ishikawa, K. Ishimori, D. Okuno, S. Nagatomo, T. Hoshino, M. Hata and N. Funasaki, *Inorg. Chem.*, 2003, **42**, 1456.
- 75 H. Meichin, K. Oohora and T. Hayashi, *Inorg. Chim. Acta*, 2018, **472**, 184.
- 76 H. Uehara, Y. Shisaka, T. Nishimura, H. Sugimoto, Y. Shiro, Y. Miyake, H. Shinokubo, Y. Watanabe and O. Shoji, *Angew. Chem. Int. Ed.*, 2017, **56**, 15279.
- 77 C. Shirataki, O. Shoji, M. Terada, S. Ozaki, H. Sugimoto, Y. Shiro and Y. Watanabe, *Angew. Chem. Int. Ed.*, 2014, **53**, 2862.
- 78 M. T. Reetz and N. Jiao, *Angew. Chem. Int. Ed.*, 2006, **45**, 2416.
- 79 T. Ueno, S. Abe, N. Yokoi and Y. Watanabe, *Coord. Chem. Rev.*, 2007, **251**, 2717.
- 80 T. Ueno, N. Yokoi, M. Unno, T. Matsui, Y. Tokita, M. Yamada, M. Ikeda-Saito, H. Nakajima and Y. Watanabe, *Proc. Natl. Acad. Sci. U. S. A.*, 2006, **103**, 9416.
- 81 J. R. Carey, S. K. Ma, T. D. Pfister, D. K. Garner, H. K. Kim, J. A. Abramite, Z. Wang, Z. Guo and Y. Lu, *J. Am. Chem. Soc.*, 2004, **126**, 10812.
- 82 M. Bacchi, G. Berggren, J. Niklas, E. Veinberg, M. W. Mara, M. L. Shelby, O. G. Poluektov, L. X. Chen, D. M. Tiede, C. Cavazza, M. J. Field, M. Fontecave and V. Artero, *Inorg. Chem.*, 2014, **53**, 8071.
- 83 I. G. Denisov, T. M. Makris, S. G. Sligar and I. Schlichting, *Chem. Rev.*, 2005, **105**, 2253.
- 84 P. Ortiz de Montellano, *Chem. Rev.*, 2010, **110**, 932.
- 85 J. Rittle and M. T. Green, *Science*, 2010, **330**, 933.
- 86 A. S. Borovik, *Chem. Soc. Rev.*, 2011, **40**, 1870.
- 87 D. P. Goldberg, *Acc. Chem. Res.*, 2007, **40**, 626.
- 88 R. Latifi, L. Tahsini, B. Karamzadeh, N. Safari, W. Nam and S. P. de Visser, *Arch. Biochem. Biophys.*, 2011, **507**, 4.
- 89 H. Srouf, P. L. Maux and G. Simonneaux, *Inorg. Chem.*, 2012, **51**, 5850.
- 90 W. Liu, X. Huang, M.-J. Cheng, R.-J. Nielsen, W. A. III Goddard and J. A. Groves, *Science*, 2012, **337**, 1322.
- 91 P. S. Coelho, E. M. Brustad, A. Kannan and F. H. Arnold, *Science*, 2013, **339**, 307.
- 92 Z. J. Wang, H. Renata, N. E. Peck, C. C. Farwell, P. S. Coelho and F. H. Arnold, *Angew. Chem. Int. Ed.*, 2014, **53**, 6810.
- 93 G. Sreenilayam, E. J. Moore, V. Steck and R. Fasan, *ACS Catal.*, 2017, **7**, 7629.
- 94 D. M. Carminati and R. Fasan, *ACS Catal.*, 2019, **9**, 9683.
- 95 R. D. Lewis, M. Garcia-Borràs, M. J. Chalkley, A. R. Buller, K. N. Houk, S. B. J. Kan and F. H. Arnold, *Proc. Natl. Acad. Sci. U. S. A.*, 2018, **115**, 7308.
- 96 K. Gruber, B. Puffer and B. Kräutler, *Chem. Soc. Rev.*, 2011, **40**, 4346.
- 97 R. Banerjee, C. Gherasim and D. Padovani, *Curr. Opin. Chem. Biol.*, 2009, **13**, 484.
- 98 K. L. Brown, *Chem. Rev.*, 2005, **105**, 2075.
- 99 R. G. Matthews, *Acc. Chem. Res.*, 2001, **34**, 681.
- 100 Y. Kung, N. Ando, T. I. Doukov, L. C. Blasiak, G. Bender, J. Seravalli, S. W. Ragsdale and C. L. Drennan, *Nature*, 2012, **484**, 265.
- 101 F. Zelder, *Chem. Commun.*, 2015, **51**, 14004.
- 102 R. G. Matthews, in *Chemistry and biochemistry of B12*, ed. R. Banerjee, John Wiley & Sons, Inc., New York, 1999, pp. 681–706.
- 103 H. P. C. Hogenkamp, G. T. Bratt and A. T. Kotchevar, *Biochemistry*, 1987, **26**, 4723.
- 104 T. Hayashi, Y. Morita, E. Mizohata, K. Oohora, J. Ohbayashi, T. Inoue and Y. Hisaeda, *Chem. Commun.*, 2014, **50**, 12560.
- 105 Y. Morita, K. Oohora, A. Sawada, K. Doitomi, J. Ohbayashi, T. Kamachi, K. Yoshizawa, Y. Hisaeda and T. Hayashi, *Dalton Trans.*, 2016, **45**, 3277.
- 106 Y. Morita, K. Oohora, E. Mizohata, A. Sawada, T. Kamachi, K. Yoshizawa, T. Inoue and T. Hayashi, *Inorg. Chem.*, 2016, **55**, 1287.
- 107 K. Oohora, N. Tang, Y. Morita and T. Hayashi, *J. Biol. Inorg. Chem.*, 2017, **22**, 695.
- 108 Y. Morita, K. Oohora, A. Sawada, T. Kamachi, K. Yoshizawa and T. Hayashi, *Inorg. Chem.*, 2017, **56**, 1950.
- 109 C.-J. Liu, A. Thompson and D. Dolphin, *J. Inorg. Biochem.*, 2001, **83**, 133.
- 110 D. Dolphin, R. L. N. Harris, J. L. Huppertz, A. W. Johnson and I. T. Kay, *J. Chem. Soc. C*, 1966, 30.
- 111 S. Scheller, M. Goenrich, R. Boecher, R. K. Thauer and B. Jaun, *Nature*, 2010, **465**, 606.
- 112 M. Krüger, A. Meyerdierks, F. O. Glöckner, R. Amann, F. Widdel, M. Kube, R. Reinhardt, J. Kahnt, R. Böcher, R. K. Thauer and S. Shima, *Nature*, 2003, **426**, 878.
- 113 M. Dey, J. Telser, R. C. Kunz, N. S. Lees, S. W. Ragsdale and B. M. Hoffman, *J. Am. Chem. Soc.*, 2007, **129**, 11030.
- 114 T. Wongnate, D. Sliwa, B. Ginovska, D. Smith, M. W. Wolf, N. Lehnert, S. Rauegi and S. W. Ragsdale, *Science*, 2016, **352**, 953.
- 115 G. K. Lahiri, L. J. Schussel and A. M. Stolzenberg, *Inorg. Chem.*, 1992, **31**, 4991.
- 116 U. E. Krone, K. Laufer, R. K. Thauer and H. P. C. Hogenkamp, *Biochemistry*, 1989, **28**, 10061.
- 117 J. Nishigaki, T. Matsumoto and K. Tatsumi, *Inorg. Chem.*, 2012, **51**, 5173.
- 118 M. W. Renner, L. R. Furenlid, K. M. Barkigia, A. Forman, H. K. Shim, D. J. Simpson, K. M. Smith and J. Fajer, *J. Am. Chem. Soc.*, 1991, **113**, 6891.
- 119 C. Brenig, L. Prieto, R. Oetterli and F. Zelder, *Angew. Chem. Int. Ed.*, 2018, **57**, 16308.
- 120 K. Oohora, Y. Miyazaki and T. Hayashi, *Angew. Chem. Int. Ed.*, 2019, **58**, 13813.
- 121 Y. Miyazaki, K. Oohora and T. Hayashi, *Inorg. Chem.*, 2020, **59**, 11995.
- 122 C. Holliger, A. J. Pierik, E. J. Reijerse and W. R. Hagen, *J. Am. Chem. Soc.*, 1993, **115**, 5651.

## ARTICLE

## Journal Name

- 123 H. Nikkila, R. B. Gennis and S. G. Sligar, *Eur. J. Biochem.*, 1991, **202**, 309.
- 124 Y. Miyazaki, K. Oohora and T. Hayashi, *J. Organomet. Chem.*, 2019, **901**, 120945.
- 125 F. Schwizer, Y. Okamoto, T. Heinisch, Y. Gu, M. M. Pellizzoni, V. Lebrun, R. Reuter, V. Köhler, J. C. Lewis and T. R. Ward, *Chem. Rev.*, 2018, **118**, 142.
- 126 J. C. Lewis, *Acc. Chem. Res.*, 2019, **52**, 576.
- 127 G. Roelfes, *Acc. Chem. Res.*, 2019, **52**, 545.
- 128 W. Ghattas, V. Dubosclard, A. Wick, A. Bendelac, R. Guillot, R. Ricoux and J.-P. Mahy, *J. Am. Chem. Soc.*, 2018, **140**, 8756.
- 129 D. J. Raines, J. E. Clarke, E. V. Blagova, E. J. Dodson, K. S. Wilson and A.-K. Duhme-Klair, *Nat. Catal.*, 2018, **1**, 680.
- 130 A. R. Grimm, D. F. Sauer, M. D. Davari, L. Zhu, M. Bocola, S. Kato, A. Onoda, T. Hayashi, J. Okuda and U. Schwaneberg, *ACS Catal.*, 2018, **8**, 3358.



Replacement of heme in an oxygen-binding hemoprotein with artificial cofactors provides artificial metalloenzymes as well as enzyme models.